Presented at the 28th European PV Solar Energy Conference and Exhibition, October 2013, Paris, France

EVALUATION AND IMPROVEMENT OF A FEATURE-BASED CLASSIFICATION FRAMEWORK TO RATE THE QUALITY OF MULTICRYSTALLINE SILICON WAFERS

Matthias Demant[1], Hannes Höffler[1], Daniel Schwaderer[2], Abrecht Seidl[3], Jonas Haunschild[1], Stefan Rein[1]
[1]Fraunhofer-ISE, Heidenhofstr 2, D-79110 Freiburg, Germany
[2]Sunways AG, Max-Stromeyer-Str. 160, 78467 Konstanz, Germany
[3]Schott AG, Technology Center Crystals, Ilmstr. 8, D-07749 Jena, Germany

ABSTRACT: The quality of multicrystalline Silicon (mc-Si) solar cells strongly depends on the quality of the wafer material. Although carrier lifetime and resistivity measurements provide basic material properties, photoluminescence (PL) images on as-cut wafers provide a much deeper insight as many crystallization defects become visible. In this work, a feature-based classification framework is introduced to rate the quality of mc-Si wafers in the as-cut stage according to the expected IV parameters of the final solar cells. For the classification, three levels of complexity are compared. In addition to frequently used PL-image features, such as dislocations and contaminated regions, physically relevant image structures are described on a wavelet basis. Beyond the improved correlation of the PL-features with quality information, the more detailed description of image structures forms a basis to understand deviations of measured and expected material quality. The classification model is evaluated within a large experiment on more than 1000 wafers, including a broad variety of wafers from different ingots and bricks from five different manufacturers, which have been processed in an industrial production line to standard solar cells with aluminium back-surface field. It is demonstrated that the presented approach allows the open circuit voltage to be predicted with a mean absolute error (MAE) of only 1.1 mV if the training of the model is performed on a random set of wafers. Moreover, the quality of wafers from an unknown ingot can be predicted with an MAE of 1.7 mV and from an unknown manufacturer still with an MAE of 3.6 mV, which proves the actual strength of the chosen approach.
Keywords: Wafer Inspection, Quality Control, Pattern Recognition, Photoluminescence

1 INTRODUCTION

The inline quality control of as-cut mc-Si wafers concerning material quality is a challenging and important step to keep low-quality wafers out of production and thus optimize cell efficiencies and production yield. Especially during the development of new solar cell concepts, an early forecast of the expected solar cell performance is necessary for the sorting of different material qualities and the separation of material- and process-related performance losses to identify necessary refinements of process parameters for further optimization. To rate the electrical quality of the wafers, the approaches using lifetime measurement or pattern recognition within PL images are the methodologies discussed most. In spite of intensive investigations in the past years, no classification method has proven so far to be able to rate mc-Si wafers from unknown manufacturers accurately.

The application of lifetime measurements via quasi-steady-state photoconductance (QSSPC) measurements [1] was investigated in [2-4]. It has been shown that for a good correlation to solar cell efficiencies, effective lifetime values from inline measurements need to be corrected with respect to trapping artefacts [5] and bulk lifetime [4], which is difficult on wafer level and difficult during an incoming control in a cell manufacturing line. PL-imaging [6] is an important technique to characterize the quality of mc-Si wafers giving spatially-resolved information on lifetime and doping. Crystal defects (e.g. grain boundaries and dislocations) and regions of reduced lifetime (e.g. contaminated region at the edges of a wafer), which arise during the crystallization process, are visible within PL-images. The correlation of these defect structures to the resulting solar cell performance was investigated in [7-10]. In addition to the basic PL-image features used in these previous works, a more advanced description of PL-images based on prototypical structures can be considered..

In addition to using the different measurement techniques separately, their results can be combined in a feature based classification framework as introduced in [8]. Based on a set of empirical data, a machine learning algorithm learns to predict the open circuit voltage given a distribution of different features on the as-cut wafers. To develop an appropriate classification scheme, a large variation of wafer materials and corresponding cell data is required. In this work, we will compare the results of three rating algorithms which will be described below.

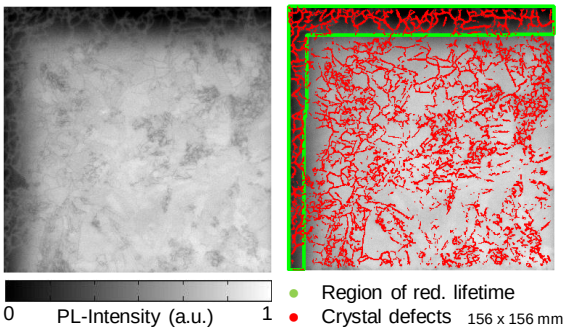

Figure 1: (Left) PL-image of an as-cut mc-Si Wafers. **(Right)** An algorithm automatically detects different features. Highlighted here are the crystal defects and contaminated edge regions.

2 FEATURE BASED CLASSIFICATION

2.1 Incoming inspection

For rating and feature classification a variety of different methods was used for the incoming inspection of wafers. The PL-images were measured as described in [7] and evaluated according to [8]. Hereby, a set of physically meaningful features observed in PL images is detected and quantified. The described image processing algorithms provide reliable results even when different fea-

tures overlap and are therefore applicable on arbitrary unsorted wafers. Dislocations and grain boundaries, for example, are also detected in regions of reduced lifetime despite the inversion of the PL signal. An exemplary detection result is shown in Fig.1.
Beyond the PL-images, the following material parameter have been measured on the as-cut wafers within the incoming inspection in the Photovoltaic Technology Evaluation Center PVTEC [12] at Fraunhofer ISE.: thickness, resistivity, carrier lifetime, micro-cracks and inclusions.
The carrier lifetime was measured by means of the quasi-steady-state photoconductance (QSSPC) technique with a WTC-100 tool from Sinton Instruments according to [1] and corrected for trapping effects [5]. The doping concentration was calculated from the resistivity which has been measured inductively by means of a Kitec PV-R tool [11]. The doping concentration and trapping-corrected carrier lifetime were added to the set of features. Inclusions and micro-cracks were measured by means of an infrared-transmission system OSIS Wafer-MicroCrack from Op-tection. The number of inclusions and micro-cracks complete the description of the wafers

2.2 Basic features

Our basic feature set contains features extracted from PL-images, IR-transmission images, as well as doping concentration and QSSPC lifetime measurements as presented in [8]. With that every wafer is characterized by a histogram of different features. Please note that this basic approach contains multiple features of different methods and is thus far more advanced than the approach to correlate single features with solar cell efficiency as it is currently introduced as a first SEMI standard for a PL-based wafer rating.

2.3 Modelling of PL-structures

It is known from literature [13], that not only the amount of defects, but also the spatial distribution of areas of reduced lifetime in the as-cut wafers affects the quality of the resulting cell. Furthermore, the combination of different defect types has an impact on the appearance of the related defect structures. This affects the quantification of defects and the interpretation of a given structure.

Within this work, combinations of local features are used to describe various structures according to their appearance in PL-images. An appropriate method to describe structures are Gabor wavelets [14]. These wavelets have a resolution in spatial and frequency domain, whereby size and frequency of the filters can be tuned to an optimal sharpness in spatial and frequency domain. Wavelet responses are extracted for different feature scales, frequency and orientations. Rotational invariance can be achieved by averaging the filter responses of a set of filters at different orientations [15]. Also, the smoothed image of dislocations or averaged PL-intensity values can be added to describe the structure within a feature vector.

In the second step, PL-structures are formed to prototypes by means of vector quantization. Hereby unsupervised clustering techniques like the k-means-clustering or self-organizing maps [16] are applied and create a so-called codebook or vocabulary of textons. These textons represent typical PL-structures. The proposed method is known as bag of features model [17] and was adapted from document retrieval to object classification. A schematic overview is depicted in Fig. 2.

To describe an image, the feature vectors are extracted for each region in the PL-image. Within a nearest neighbour search, the feature vectors are mapped onto the best matching prototype. Finally each wafer can be described by the distribution of typical PL-structures in its PL-image, a histogram over the defined vocabulary and prototypes, respectively.

2.4 Extended feature set

A third extended feature set is formed, if the description from basic features and prototypes is combined. Therefore three different approaches (i) via basic features and (ii) via prototypes and (iii) their combination will be compared. The results from this rating are used to predict *global* solar cell parameters (here: V_{OC}). The prediction of *local* solar cell parameters (e.g. J_0) was presented elsewhere [18].

2.5 Classification via SVM

For all feature sets, our approach is based on the evaluation of a large amount of empirical data. After the training set of wafers is described by the three feature sets measured at wafer level, a supervised machine learning algorithm learns to predict the quality of the wafer based on the cell results, achieved on the solar cells which have been manufactured from the training wafers. The model has to be evaluated on unknown data to test its

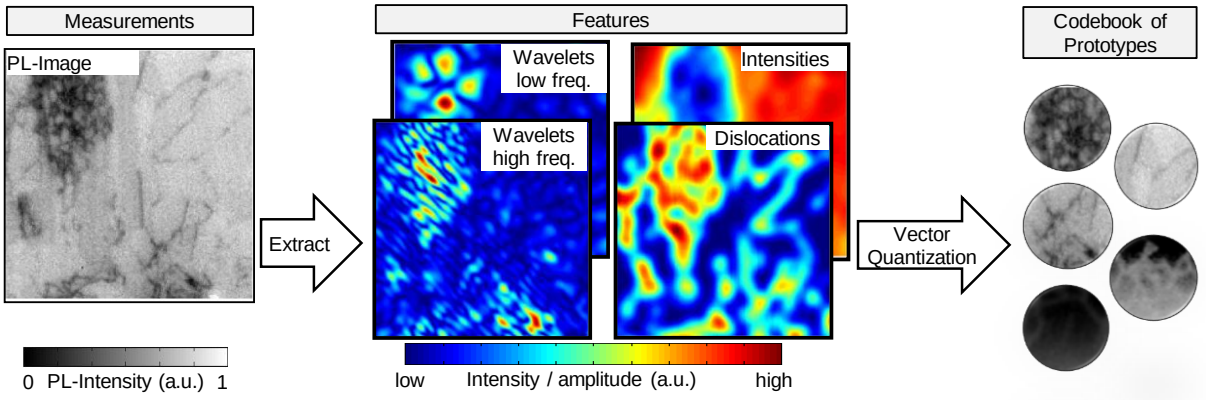

Figure 2: Schematic overview of the generation of the codebook of prototypes. Using wavelets, different features are extracted from a PL image. The combination of several local features forms a prototype and the wafer can be described by a set of prototypes found in the codebook.

quality. A frequently occurring challenge is an overfitting of the model to the given training data. Therefore support vector machines (SVM) are used. SVMs are supervised learning models which classify input data with a focus on a high generalization performance of the model. Based on the kernel trick, the algorithm maps the input data into higher dimensional space. Within the classification step, an optimal hyperplane is trained which maximizes the margin between the classes. The classifier acts linear in the higher dimensional space, but may be nonlinear in the original space. A brief historical background of SVMs and a description of SVM regression is given in [19]. Within this work, Vapnik's ε-SV regression model, as described in [19, 20], is trained with a radial basis kernel to predict the open circuit voltage.

3 MATERIAL SELECTION

Within our experiment a large variety of different material types has been investigated. 781 wafers from 12 bricks of 8 ingots and 2 manufacturers and 254 wafers taken out of 40 different boxes of 6 additional manufacturers were selected. The wafers which were taken from ingots were chosen from different positions within the ingot and brick, with a distance in brick height of at least 10 wafers. The wafer sets from bricks also contained wafers from top and bottom regions of the bricks as far as these wafers came from brick regions which fulfilled the standard cut-off criterion of a brick-lifetime above 2 µs measured via µPCD from Semilab.

After finishing the measurements on wafer-level, the images and global data were analysed and three sets of features extracted. First, the set of *basic features* was computed according to section 2.2. In a second feature set of *prototypes*, the basic PL-features were replaced by PL-structures. Therefore, a codebook of 25 prototypical PL-structures was modelled according to section 2.3. In a third *extended* set of features, a combination of basic features and typical PL-structures (section 2.4) was combined.

The whole set of wafers was processed to solar-cells with aluminium back-surface field (Al-BSF) in an industrial production line at Sunways. After solar cell production, current-voltage *(IV)* measurements were performed. Based on open-circuit voltage and the described features, a classification scheme was trained to rate the quality of the wafers applying Chang's libsvm implementation [21]. Before a classification scheme can be used, it needs to be trained. Within our experiment, training and test set are split according to different configurations.

In our first configuration, the instances are randomly split into training and test set and evaluated according to three different feature combinations. To avoid an overfitting of the data a 3-fold cross-validation is applied. All instances are divided into three groups. Each group is predicted based on the training with the remaining groups.

The second configuration investigates the prediction quality of wafers taken from an unknown ingot. A set of 164 wafers from 3 different bricks are excluded from the training set. The model is trained with a 3-fold cross-validation on the remaining wafers. I.e., none of the wafers of the unknown ingot is trained.

In a third configuration the degree of similarity between wafers in test and training set is further reduced. This time all 344 wafers of a specific manufacturer are removed from the training set. Our prediction model is evaluated on wafers of this "unknown" manufacturer.

4 RESULTS

The prediction quality of the model is evaluated based on the correlation coefficient r^2, the mean absolute error (MAE) and the root mean squared error (RMS). Exemplary prediction results for varying combinations of datasets and feature sets are listed in table 1. Chosen results are depicted in Fig.3

Table I: Quality of prediction models based on varying data and feature sets.

Prediction . (#test/training)	Feature	Corr. coeff.	MAE. [mV]	RMS [mV]
Rand.mixture	Basic feat.	0.89	1.6	2.5
(3-fold)	Prototypes	0.92	1.4	2.2
	Ext. feat.	0.94	1.1	1.8
Ingot	Basic feat.	0.89	2.0	2.7
(164/779)	Prototypes	0.88	2.3	3.0
	Ext. feat.	0.89	1.7	2.4
Manufacturer	Basic feat	0.74	3.1	4.1
(344/599)	Prototypes	0.78	3.7	4.3
	Ext. feat.	0.75	3.6	4.5

The prediction results for random selection shows good correlations for both the basic and the extended approach. Especially the extended approach leads to very good results, keeping in mind that process fluctuations and accuracy of the IV measurement can add up to an error of approximately 2 mV.

If wafers from an unknown ingot are predicted, again the extended features show best results. Strongly misclassified wafers (e.g. the most left data points in Fig 3 middle row) can be identified by their wafer ID, which allows to select and analyse unprocessed sister wafers in order to find the cause for the misclassification and to further improve the rating model. This will be done in the next step.

The prediction of an unknown manufacturer increases the mean absolute prediction error above 3 mV. Results of further "unknown" manufacturers show prediction results of similar or slightly reduced quality with overall mean prediction errors of 3.2 mV for basic features, and 3.9 mV for the prototype or extended feature set.

5 DISCUSSION

The quality of a learning-based classification scheme depends on the extent and the distribution of the given data. The evaluation based on a random selection of wafers shows very good prediction results. Comparable open-circuit voltages are assigned to wafers with similar signatures. The description of the wafers is refined using PL-structures instead of basic features. Also adding PL-structures to the feature vector leads to an improved prediction quality. The high precision of the prediction can be referred to the smooth transitions in wafer signature and quality within a brick.

The prediction of wafers of an unknown ingot leads to prediction results with MAE of 2 mV. Considering that natural process deviations and measurement errors are in the same range, this is an excellent result which confirms our approach. A quality prediction of material of an unknown manufacturer compared to a known manufacturer

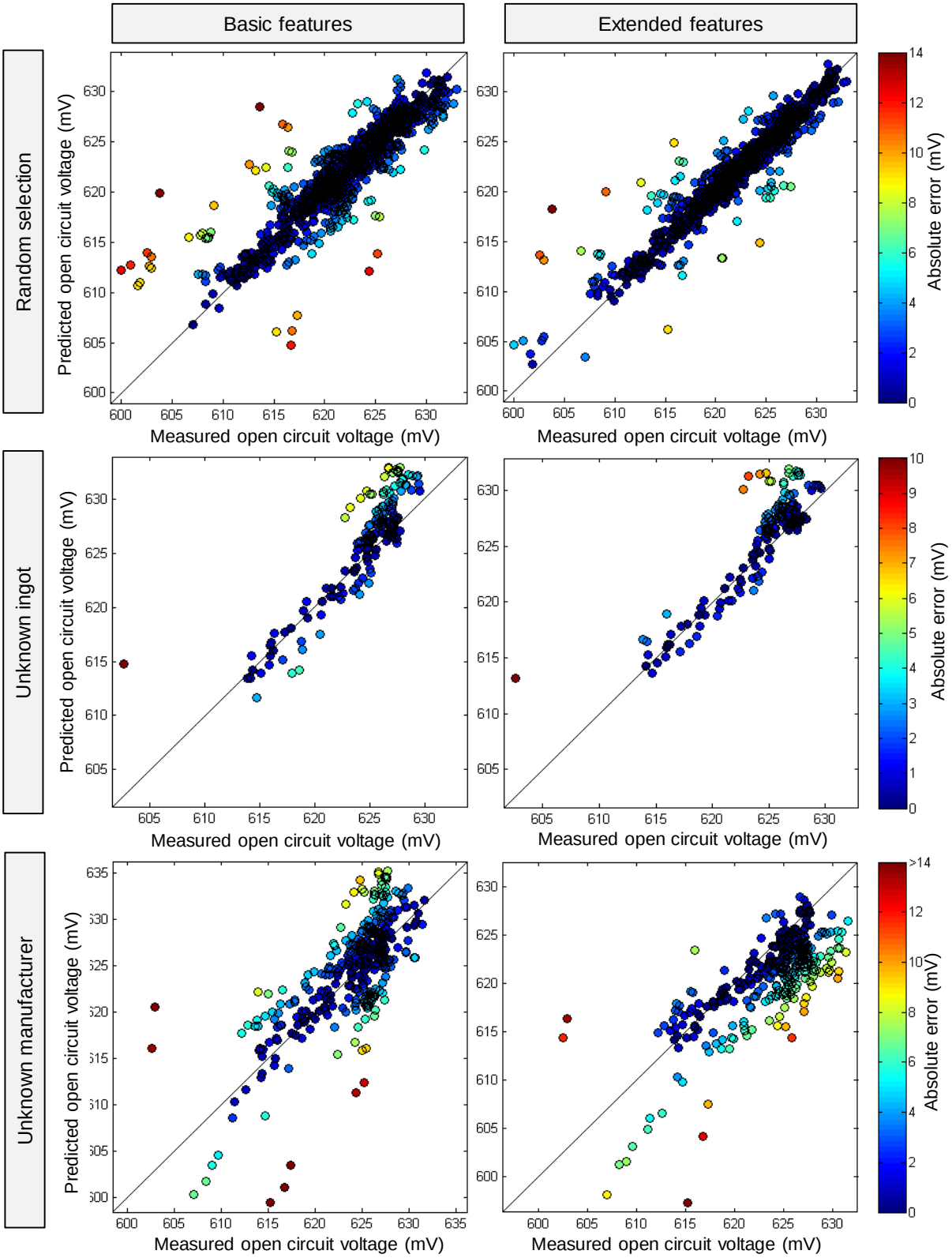

Figure 3: Prediction results for varying training and test configurations (rows) based on different feature combinations (columns). The plots show measured and predicted open-circuit voltages with a random split of training and test data (top row), a test of 164 wafers from 3 bricks of an unknown ingot (middle row) and the prediction of an unknown manufacturer. In all approaches the models were trained with a SVM using a 3-fold cross-validation to avoid an over-fitting of the data to the test set. Especially the prediction results of wafers from an unknown ingot confirm our approach.

shows a reduced performance. This may originate from different characteristics of the unknown material. Despite the high generalization performance of the SVM, an extrapolation of the prediction model to data with strongly varying characteristic can lead to misclassifications. Moreover, an unbalanced distribution of the data can lead to an unwanted bias within the prediction model.

Fig. 4 depicts the open-circuit voltage (V_{oc}) distribution of the training set (red bars) and of the test set of the predicted unknown manufacturer (green bars). Wafers from the unknown manufacturer show higher V_{oc} values compared to the training set. Concurrent, the visualization in Fig. 3 (third row, right column) for the wafers from an unknown manufacturer predicted with an extended feature set appears to underestimate the wafer quality. Due to additional structural information, the extended feature set leads to a more detailed description of the wafers and may be more sensitive to strongly imbalanced distributed test and training data. We expect that more empirical observations with a broad set of material will lead to a higher classification performance.

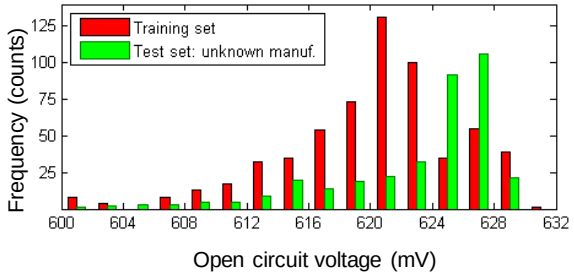

Figure 4: Distribution of the measured open-circuit voltages of training and test set. Bins are given in steps of 2mV.

7 CONCLUSION & OUTLOOK

To improve the rating and prediction results of the quality of mc-Si wafers in terms of the final solar cell parameters, three feature-based approaches were developed and compared. The first basic feature set consists of scalar values extracted from various inline measurements during inline inspection, including e.g. features from PL and IR images. The second feature set consists of prototypes of special PL structures which are generated via wavelet features and quantized in a codebook. The third feature set is the combination of the basic set and the prototype set. Using a support vector machine, the rating was trained in different combinations of wafer sets and rating approach. On a material basis of approx. 1000 precisely characterized wafers, all approaches yielded errors being only slightly higher than measurement errors and process deviations. Completely unknown material could be predicted with only slightly reduced accuracy. As a result, the feature based rating is a very promising approach to further improve rating algorithms based on the correlation of single features.

In the next steps, prediction errors of unknown manufactures are going to be examined in more detail. The modelled PL-structures can be used to evaluate differences in the distribution of crystal defects in bricks and ingotss of different manufacturers. A first approach to model relevant structures in photoluminescence images was introduced in [18]. Considering the local dark saturation current as a spatially resolved quality measure, the understanding and selection of PL-structures can be improved.

7 ACKNOWLEDGMENTS

We thank the team of Schott Solar Wafer for the detailed material selection, the PV-TEC Team at Fraunhofer ISE for extensive characterization of the wafers during incoming inspection and the team from Sunways for solar cell processing. This work has been supported by the German Ministry for Education and Research (BMBF) under the frame of the project “Q-Wafer” (03SF0409A and B).

8 REFERENCES

[1] R.A. Sinton, & A. Cuevas, Applied Physics Letters 69 (1996) 2510.
[2] K. Bothe, R. Krain, R. Falster, et al., Progress in Photovoltaics: Research and Applications 18 (2010) 204.
[3] N. Enjalbert, F. Coustier, N. Le Quang, et al., Barcelona, Spain, Barcelona, Spain (2005) 1124.
[4] R.A. Sinton, J. Haunschild, M. Demant, et al., Progress in Photovoltaics: Research and Applications (2012) 1.
[5] D. Macdonald, R.A. Sinton, & A. Cuevas, Journal of Applied Physics 89 (2001) 2772.
[6] T. Trupke, & R.A. Bardos, Orlando, USA, Orlando, Florida, USA (2005) 903.
[7] J. Haunschild, M. Glatthaar, M. Demant, et al., Solar Energy Materials & Solar Cells 94 (2010) 2007.
[8] M. Demant, M. Glatthaar, J. Haunschild, et al., Valencia, Spain, Valencia, Spain (2010) 1078.
[9] T. Trupke, J. Nyhus, & J. Haunschild, Physica Status Solidi RRL (2011) published online.
[10] B. Birkmann, A. Hüsler, A. Seidl, et al., Proceeding of the 26th EU-PVSEC, Hamburg, Germany (2011) 1.
[11] M. Spitz, U. Belledin, & S. Rein, Milan, Italy, Milan, Italy (2007) 47.
[12] D. Biro, R. Preu, S.W. Glunz, et al., Dresden, Germany, Dresden, Germany (2006) 621.
[13] J. Isenberg, J. Dicker, & W. Warta, Journal of Applied Physics 94 (2003) 4122.
[14] J.G. Daugman, Acoustics, Speech and Signal Processing, IEEE Transactions on 36 (1988) 1169.
[15] H. Schulz-Mirbach, DAGM - Symposium Mustererkennung, (1995) 1.
[16] T. Kohonen, M.R. Schroeder, & T.S. Huang, Self-Organizing Maps, 3rd ed., Springer-Verlag New York, Inc., Secaucus, NJ, USA, 2001.
[17] J. Sivic, & A. Zisserman. in Proceedings of the Ninth IEEE International Conference on Computer Vision - Volume 2, pp. 1470, IEEE Computer Society 2003.
[18] M. Demant, J. Greulich, M. Glatthaar, et al., Energy Procedia 27 (2012) 247.
[19] A.J. Smola, & B. Schölkopf, Statistics and Computing 14 (2004) 199.
[20] V. Vapnik, The Nature of Statistical Learning Theory, Springer 1995.
[21] C.-C. Chang, & C.-J. Lin, ACM Trans. Intell. Syst. Technol. 2 (2011) 1.